Preprint Title Finite Element Analysis of Graphene Oxide Based Nanoelectromechanical Capacitive Switch

Authors Rekha Chaudhary and Prasantha R. Mudimela

Publication Date 12 Aug 2019

Article Type Full Research Paper

ORCID® iDs Rekha Chaudhary - https://orcid.org/0000-0002-5804-2962;
Prasantha R. Mudimela - https://orcid.org/0000-0001-5788-4183

Finite Element Analysis of Graphene Oxide Based Nanoelectromechanical Capacitive Switch

Rekha Chaudhary, Prasantha R. Mudimela*

School of Electronics and Electrical Engineering, Lovely Professional University, Jalandhar, India - 144411

Email: Prasantha Reddy Mudimela*- prasantha.22708@lpu.co.in

*Corresponding author

Abstract

The present work deals with finite element analysis (FEA) of a novel configuration of double clamped nanoelectromechanical (NEM) capacitive switch. Graphene oxide (GO), a graphene derivative has been used as suspended beam material in NEM switch for the first time. In the proposed work, GO is used as dielectric material having negative Poisson's ratio value. The variation in capacitance has observed as the beam is pulled down by the actuating electrode. Analysis of pull-in voltage and von Mises stress are done using COMSOL Multiphysics, for standard and perforated GO NEM switch structures. The actuation voltage of 5.4 V for standard beam structure and 3.35 V for perforated beam structure have been achieved for the beam length of 1µm and width of 0.3 µm. The actuation voltage and von Mises stress value have reduced by making perforations in the beam. The comparative analysis of graphene and GO NEM switches have also been done in terms of von Mises stress to ensure the mechanical reliability. The von Mises stress values for GO NEM switch and graphene NEM switch are 500 MPa and 4.8 GPa respectively. This lesser value of von Mises stress in GO NEM switch makes it a good choice as beam material. The capacitive switch is demonstrated for standard and perforated beam structures. The variation in capacitance has observed as the beam is pulled down by the actuating electrode and at actuation voltage, the maximum value of capacitance obtained is 0.9403 pF.

Keywords

capacitance effect; FEM simulation; graphene oxide; NEM switches; von Mises stress;

Introduction

In the era of miniaturization, NEM switches can easily set back the already existing conventional switches due to some outstanding properties like extremely small size, sharp switching, low leakage current and large capacitance ratio [1] [2]. For applications like logic gates and data storage, NEM switches can be used [3]. Already existing metal switches suffers from the problem of stiction, self-actuation and electro migration [4]. Graphene NEM switches overcome the stiction problem with better reliability [5]. Graphene based NEM switches offers lower pull-in voltage and fast switching speed [6]. But Graphene NEM switches suffers from the problems like structural deformation and low life cycle (500 cycles) [7]. Very high young's modulus of graphene beam makes beam stiffer and due to repetitive on-off switching of NEM switch, structural deformation take place.

GO is graphene derivative that can be semiconductor or an insulator, depending on the degree of oxidation [8]. Physical and mechanical properties of GO can be changed by changing the degree of oxidation [9]. Rippling in GO can alter the mechanical characteristics of the material [10]. In GO, on increasing the oxidation rate Poisson's ratio decreases linearly. For fully oxidized GO, value of Poisson's ratio is negative [11]. Young's modulus value of GO is 27-31GPa which is much lower than Young's modulus value of graphene 1TPa [12][13]. This lesser value makes beam less stiff and more flexible. The high stiffness of GO is associated with an unexpected low bending modulus and makes it super flexible [14]. GO can be used in application like sensors [15][16], capacitors [17], transparent conductors [18] and water purification [19][20] etc.

Actuation voltage is an important parameter in NEM switches, which directly depends upon the spring stiffness of beam, gap between actuation electrode and beam [21]. Spring constant of double clamped beam depends upon Young's modulus of beam material and thickness of beam [22]. Actuation voltage can be reduced by using any one of the methods: reduce young's modulus, reduce thickness of beam or use perforated beam [23].

NEM switch actuation can be done using different methods like electrostatic [24] [25], thermal [26], piezoelectric [27] and magnetic [28]. But electrostatic actuation is the most favourable actuation mechanism as it requires low power consumption, small electrode size and low switching time. Electrostatic actuation mechanism was achieved by applying voltage at bottom graphene electrode and ground potential at top graphene electrode. When applied voltage is lesser than pull-in voltage, the beam remains in up-ward direction and this state is called as off state. But, when applied the voltage exceeds pull-in voltage, electrostatic actuation mechanism pulls the beam downward and touches the actuating electrode. This state is known as on state.

In the proposed work, FEA of GO based NEM switches have been investigated for the first time. The capacitive effect has been reported for the novel configuration of NEM switch in on state switching. The 3D switch designing of GO NEM switches have been done in COMSOL Multiphysics version 5.4. Pull-in response analysis and von Mises stress analysis have been carried out in finite element method (FEM) simulation.

Device geometry description

This section describes the geometrical dimensions of NEM switch. Use of GO as a dielectric has been proposed in the NEM switch configuration. For the operation of NEM switch, two graphene electrodes were used. One graphene electrode (actuator) was situated under the GO beam (5 nm thick) and other graphene electrode (3 nm thick) was placed just above the GO beam. In FEM simulations, GO (dielectric) was used as beam material and two graphene electrodes were used one as actuating electrode, other as ground electrode. The simulations were performed for both standard and perforated beam structures. The simplified diagram of double clamped GO NEM switch is illustrated in Figure 1. The top view of perforated GO beam is illustrated in Figure 2.

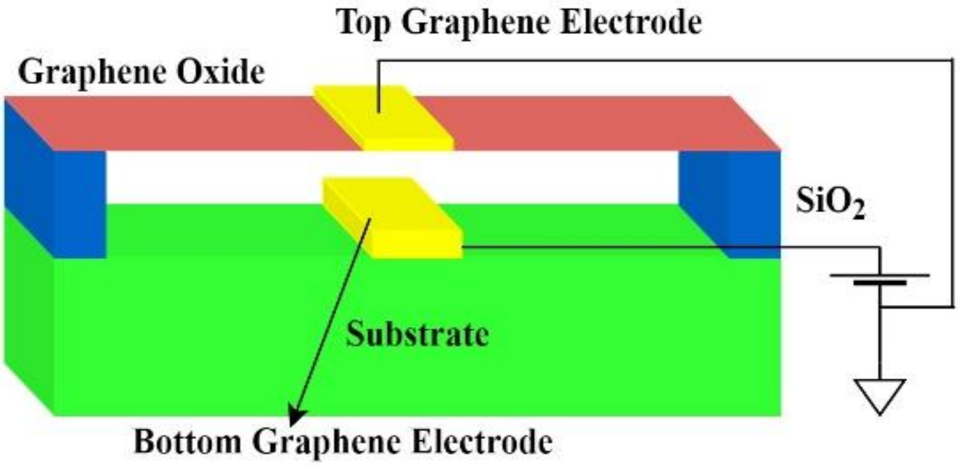

Figure 1: Simplified figure of GO NEM switch.

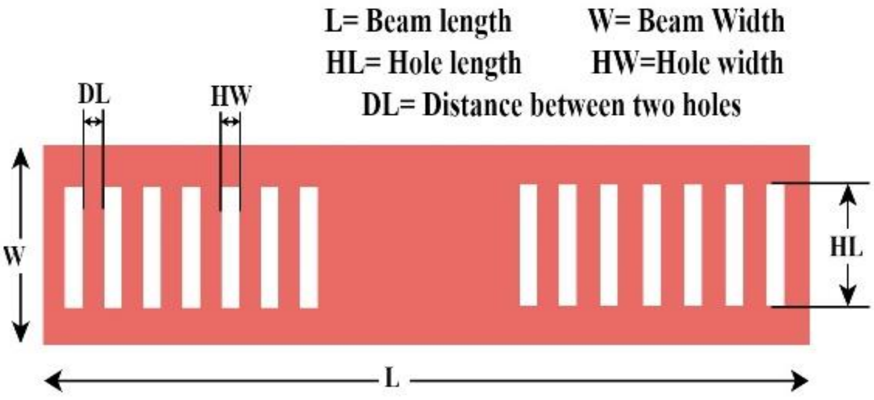

Figure 2: Top view of perforated GO beam.

The suspended beam dimensions of GO NEM switch are given in table 1 and perforated GO NEM switch dimensions are given in table 2.

Table 1: Dimensions of beam material for FEM simulation.

Design parameters	**Values**
Beam Material	GO
Total beam width	0.3 µm
Total beam length	1 µm
Beam Thickness	2.8 nm
Gap between beam and electrode	30 nm
Electrode area (L*W)	200 nm* 300 nm

Table 2: Dimensions of perforations of GO beam material for FEM simulation

Perforations parameters	**Values (nm)**
Distance between two holes (DL)	80
Hole length (HL)	30
Hole width (HW)	200

FEM Modelling

Double clamped NEM shunt switch using GO as beam material was simulated in COMSOL Multiphysics version 5.4. For the first time, GO has been used as beam material in NEM switches. To evaluate the pull-in and von Mises analysis, electromechanics module was used. For all FEM simulations, GO Young's modulus was set to 27GPa and Poisson's ratio value was set to -0.567 [11]. Free tetrahedral triangular mesh was used to reduce meshing complexity. In air medium at 1 atm pressure, suspended GO beam was positioned on the top at a distance of 30 nm from the bottom graphene electrode. The strong adhesion between graphene and GO supports the bonding of upper graphene electrode and suspended GO beam. For top electrode, graphene beam was positioned just above the GO beam and was kept at 0V. While electric potential was applied to the bottom graphene actuating electrode. All remaining boundaries were electrically insulated. For comparative analysis, FEM simulations for graphene based NEM switch were also done by taking the same device dimensions.

Results and Discussion

In this paper, simulations of NEM switches have been performed by taking GO as beam material using FEM based tool. To compare the results with GO NEM switch, simulations of graphene NEM switch were also performed.

Figure 3 illustrates the results of von Mises stress analysis for standard and perforated graphene NEM switch structures. The obtained von Mises stress values for the case of graphene and perforated graphene NEM switches are 4.8 GPa and 3.86 GPa respectively. The von Mises stress occurs maximum at the beam edges and minimum at the beam center. The von Mises stress is very high (GPa) in graphene NEM switch. So, the beam is replaced by GO beam along with graphene.

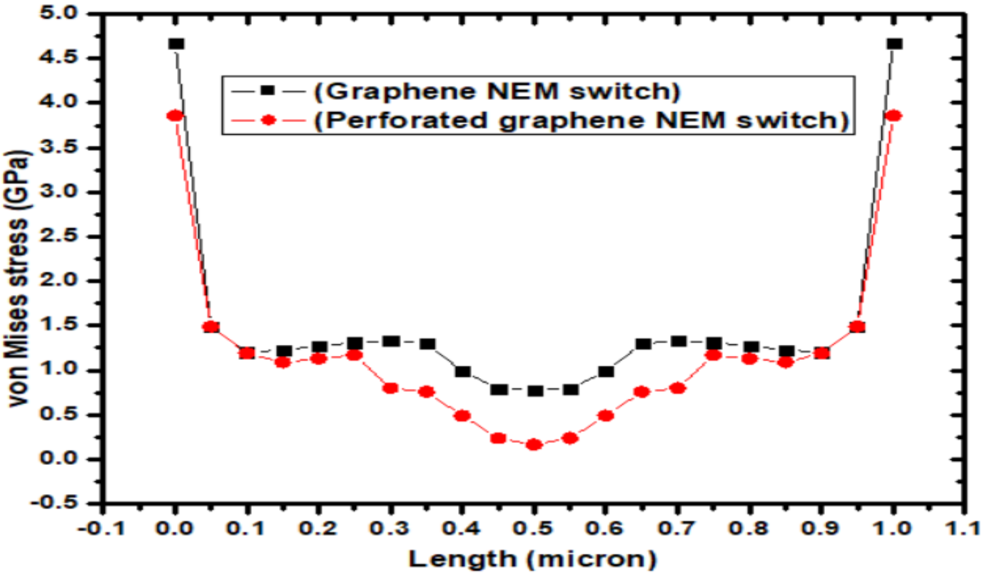

Figure 3: The von Mises stress of graphene NEM switch with and without perforations.

GO NEM switch standard and perforated beam structure

For the device dimensions mentioned in table 1, actuation voltage of 5.4 V and von mises stress of 500 MPa was achieved. Figure 4, shows the total displacement when beam was in contact with the actuating electrode due to actuation mechanism.

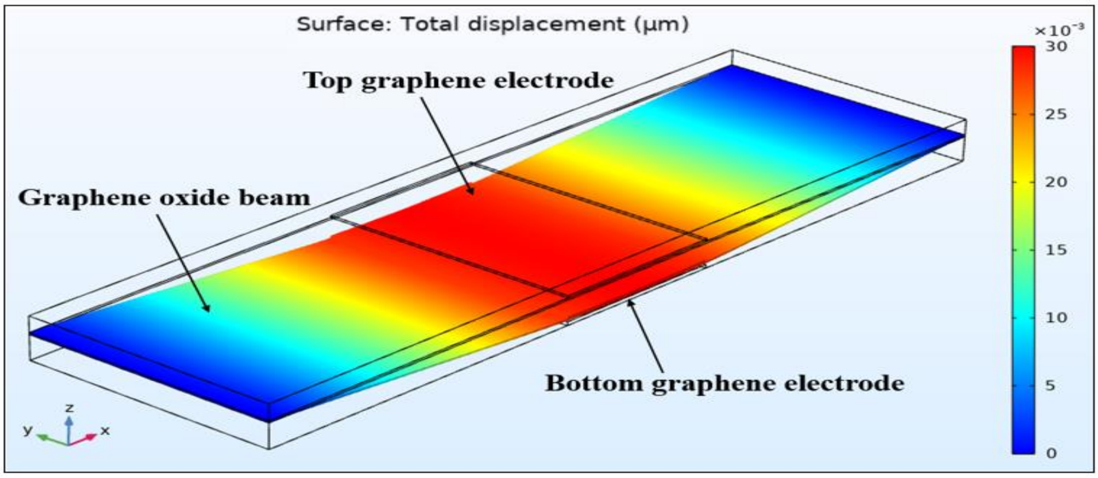

Figure 4: Schematic diagram of standard beam structure in down state.

To observe the effect of introducing holes into the beam, FEM simulations of perforated GO beam were performed as shown in figure 5. For the device dimensions mentioned in table 2, actuation voltage of 3.35 V and von Mises stress of 419 MPa was obtained. The pull-in voltage was reduced to 3.35 V from 5.4 V (without perforations) by introducing perforations into the beam.

The results show that making perforations into the suspended GO beam of NEM switch reduces both, pull- in voltage and von Mises stress. Due to perforations, air below the suspended beam get easily squeezed out when the beam is pulled down by actuating electrode. Hence reduces pull-in voltage.

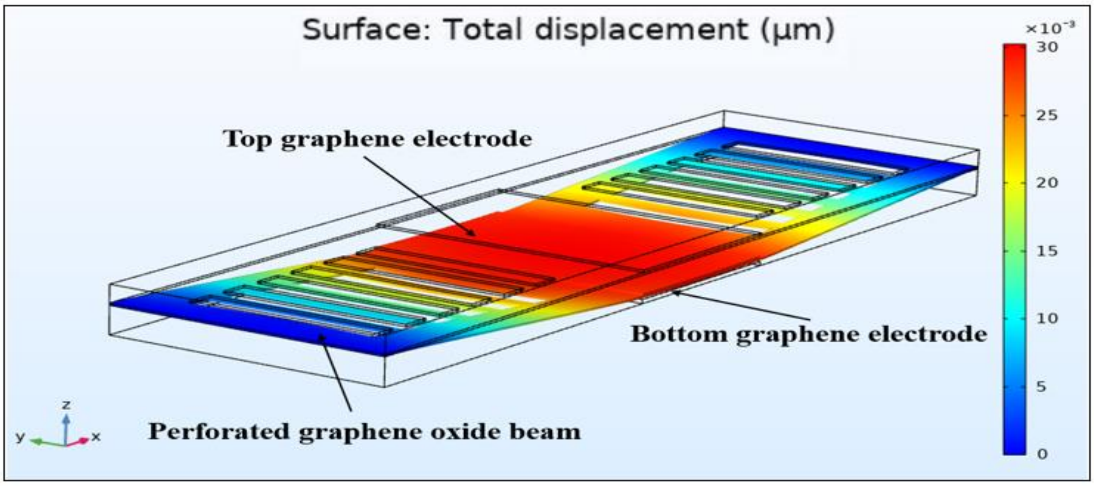

Figure 5: Schematic diagram of perforated beam in down state.

The change in von Mises stress along the beam length for both the GO NEM switch structures is shown in figure 6. In standard beam structure, von Mises stress is maximum (500 MPa) at the beam edges and at the beam center edges. But for perforated beam structure, von Mises stress is maximum (419 MPa) only at the beam edges and at center it is having lesser value (228 MPa). At center, this value is almost half of the value of maximum von Mises stress in case of standard beam structure. Perforated beam structure reduces the von Mises stress acting on suspended beam. In both cases, von Mises stress follow a specific trend. At beam edges and at the beam center, von Mises stress is high but in between the edge and the center of beam, von Mises stress value is low.

In GO and graphene NEM switch, maximum von Mises stress occur at corner of beams. Interestingly we have observed that for GO NEM switch, von Mises stress again increases at the beam center. This rise in von Mises stress is due to the presence of upper graphene electrode. The interface at which graphene is situated above GO beam suffers higher stress, as the beam at the center is thicker than the corner beam.

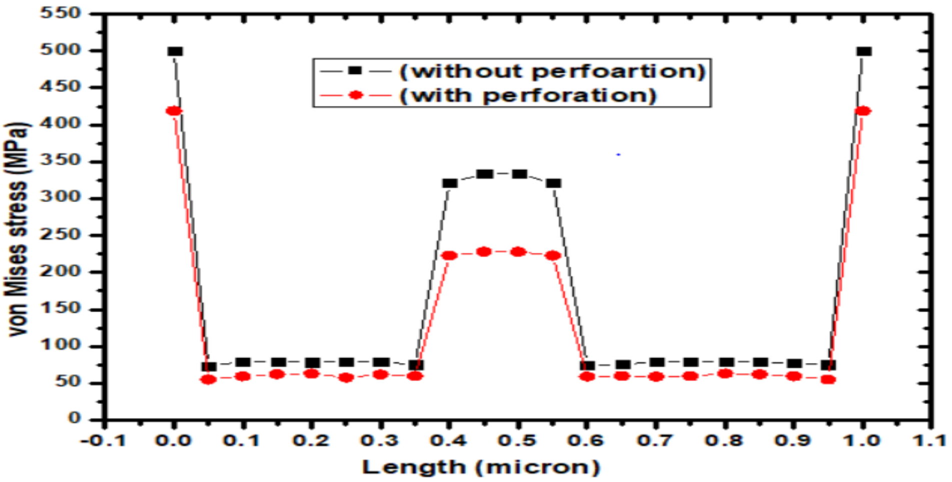

Figure 6: The von Mises stress of GO NEM switch with and without perforations.

In graphene NEM switch, the maximum von Mises stress is 4.8 GPa while for GO NEM switch von Mises stress is 500 MPa. The von Mises stress in GO NEM switch is almost ten times lower than stress in graphene NEM switch.

Figure 7. shows the top view of von Mises stress contour plot of both standard and perforated beam structures. In standard beam structure, maximum stress occurs at beam corners and at the beam center edges while in case of perforated structure, maximum stress occurs at the beam corners and at the perforation’s edges. The edges of the beam suffer maximum stress in both cases because electric field strength is very intense at the beam edge.

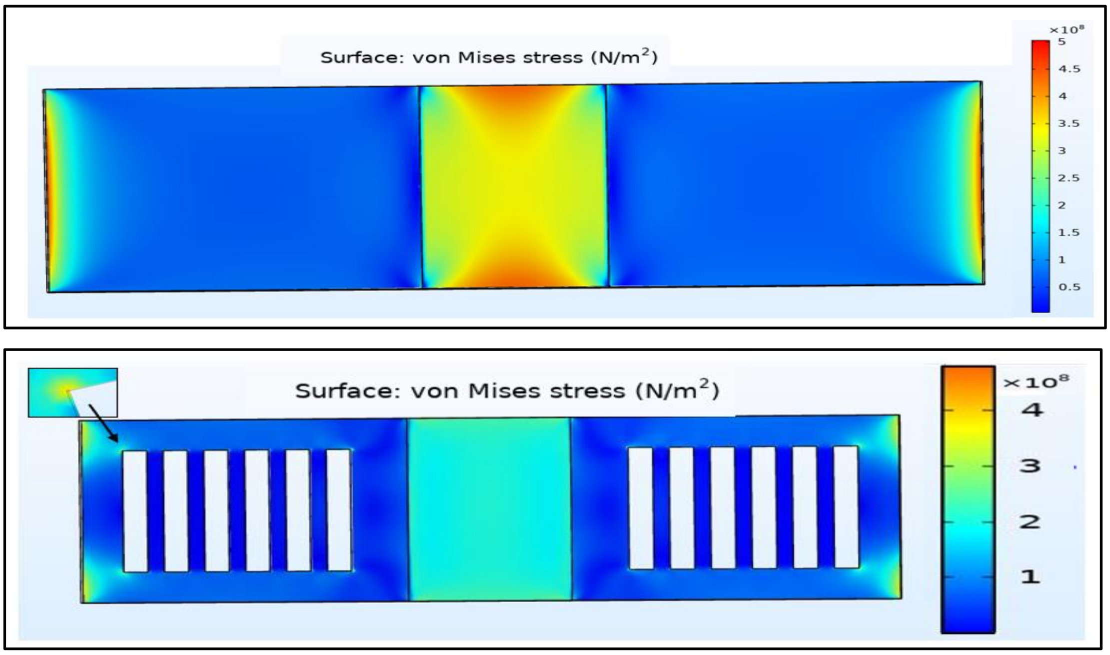

Figure 7: Contour plot of von Mises stress for standard and perforated GO beam structure.

In comparison of both graphene and GO NEM switches, it is concluded that GO based NEM switch withstand less von Mises stress than graphene NEM switch. So, the choice of GO as beam material over graphene is good. Since the results illustrate that perforated beam structure requires less actuation voltage and withstand less von Mises stress effect (at center), perforated GO beam NEM switch is more reliable than standard GO beam NEM switch.

From off state to on state of NEM switch, variation in capacitance has been encountered as 3 nm thick graphene layer was used just above GO. Depending upon the applied voltage, the distance between GO beam and bottom graphene electrode changes. At actuation voltage, when the beam touches the actuation electrode it forms capacitor structure. In NEM switch, down state capacitance is the sum of parallel plate capacitance (C_p) and fringing field capacitances (C_f) as shown in figure 8.

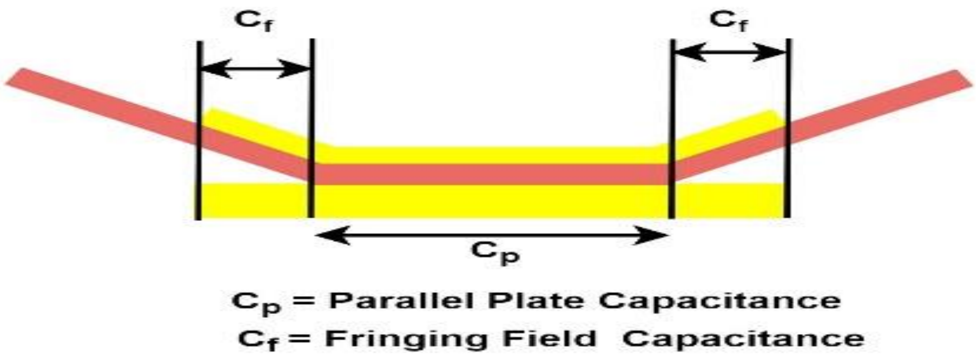

Figure 8: Total capacitance in down state.

As shown in figure 8, the slanting position of GO beam with bottom electrode gives fringing capacitance (C_f). The simulated results for fringing field capacitance are evaluated by integrating the capacitance values from parallel plate capacitor edge to bottom electrode edge. The value of C_f obtained on both sides ($2C_f$) is 359.2 aF. The simulated value of down state capacitance (C_d=C_p+$2C_f$) is 0.9403 pF.

In figure 9, results of variation in capacitance value with varying applied voltage are presented for both standard and perforated GO NEM switch. The voltage variation is done from 0.9 V to 5.4 V for standard GO NEM switch. It results in variation in gap from 23 nm to 0 nm. For perforated structure, voltage variation is done from 0.9 V to 3.35 V that varies the gap from 20 nm to 0 nm. As the applied voltage is increased, due to the effect of electrostatic force, the beam gets pulled down towards the electrode and gap between the beam and electrode decreases. When the applied voltage is varied, the gap between beam and electrode changes, in response to that different values of capacitance are obtained. When the applied voltage is equals to the actuation voltage, the beam snaps down by the electrode and forms a capacitor structure. In standard and perforated GO NEM switches, total capacitance obtained is 0.9403 pF when GO completely in contact with bottom electrode. As the device dimensions are same for both the cases including GO, total capacitance is same at actuation voltages 5.4 V for standard and 3.35 V for perforated GO NEM switches.

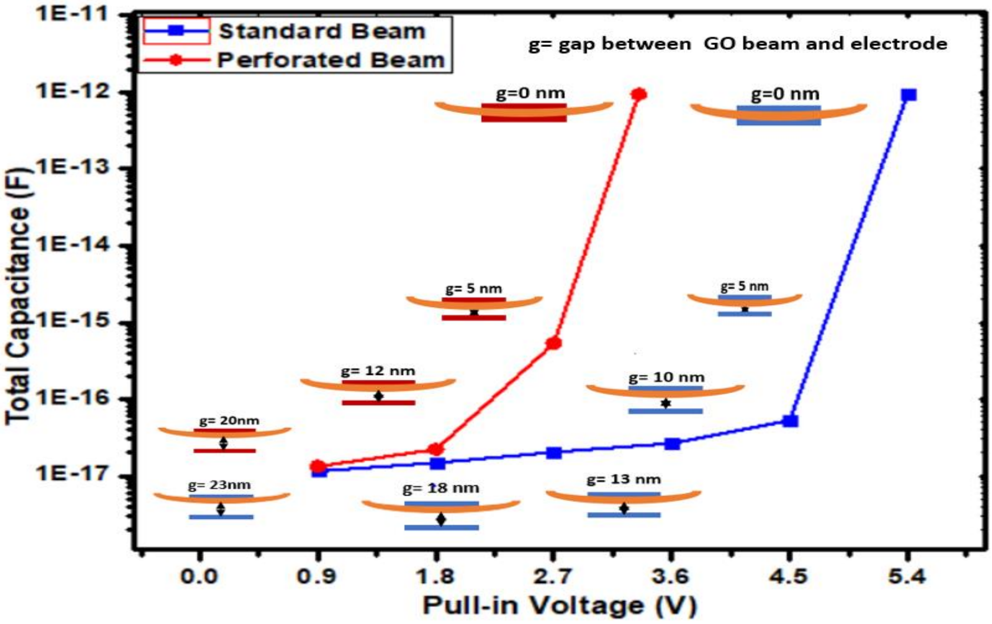

Figure 9: Variation in Capacitance plot for standard and perforated GO NEM Switch.

Conclusions

In this work, the pull-in response and mechanical reliability of GO based NEM switch was investigated for the first time. The reported work presents a novel configuration of NEM capacitive switch using GO beam along with graphene beam as suspended bridge material. Based on finite element analysis of both standard and perforated GO NEM switches, the perforated beam structure is preferred over standard beam structure as it requires low pull-in voltage. Moreover, the von Mises stress comparative analysis of GO NEM switch and graphene NEM switch exhibits that GO is a better choice for beam material as GO NEM switch withstand less von Mises stress than graphene NEM switch. The variation in capacitance was successfully demonstrated when the suspended beam actuated towards the bottom graphene electrode. The maximum value of capacitance obtained was 0.9403 pF when GO beam was in contact with bottom electrode. The proposed structure, GO based NEM switch could be used for data storage and memory applications.

References

[1] Loh, O.Y.; Espinosa, H. D. Nature Nanotechnology, **2012**, 7, 283-295.

[2] Kim, J. H.; Chen, Z. C.; Kwon, S.; Xiang, J. Nano Letters, **2014**, 14, 1687-1691.

[3] Loh, O.; Wei, X.; Sullivan, J.; Ocola, L. E.; Divan, R.; Espinosa, H. D. Advanced Materials, **2012**, 24, 2463-2468.

[4] Jhanwar, P.; Bansal, D.; Pandey, S.; Verma, S.; Rangra, K. J. Microsystem Technologies, **2015**, 21, 2083-2087.

[5] Milaninia, K. M.; Baldo, M. A.; Reina, A.; Kong, J. Applied Physics Letters, **2009**, 95, 183105.

[6] Sharma, P.; Perruisseau C. J.; Moldovan, C.; Ionescu, A. M. IEEE Transactions on Nanotechnology, **2013**, 13, 70-79.

[7] Shi, Z.; Lu, H.; Zhang, L.; Yang, R.; Wang, Y.; Liu, D.; Guo, H,; Shi, D.; Gao, H.; Wang, E.; Zhang, G. Nano Research, **2012**, 5, 82-87.

[8] Inagaki, M.; Kang, F. Journal of Materials Chemistry A, **2014**, 2, 13193-13206.

[9] Krishnamoorthy, K.; Veerapandian, M.; Yun, K.; Kim, S. J. Carbon, **2013**, 53, 38-49.

[10] Shen, X.; Lin, X.; Yousefi, N.; Jia, J.; Kim, J. K. Carbon, **2014**, 66, 84-92.

[11] Wan, J.; Jiang, J. W.; Park, H. S. Nanoscale, **2017**, 9, 4007-4012.

[12] Cao, C.; Daly, M.; Singh, C. V.; Sun, Y.; Filleter, T. Carbon, **2015**, 81, 497-504.

[13] Sun, J.; Schmidt, M. E.; Muruganathan, M.; Chong, H. M.; Mizuta, H. Nanoscale, **2016**, 8, 6659-6665.

[14] Poulin, P.; Jalili, R.; Neri, W.; Nallet, F.; Divoux, T.; Colin, A.; Aboutalebi, S. H.; Wallace, G.; Zakri, C. Proceedings of the National Academy of Sciences, **2016**, 113, 11088-11093.

[15] Huang, X.; Yin, Z.; Wu, S.; Qi, X.; He, Q.; Zhang, Q.; Yan, Q.; Boey, F.; Zhang, H. Small, **2011**, 7, 1876-1902.

[16] Liu, Y.; Dong, X.; Chen, P. Chemical Society Reviews, **2012**, 41, 2283-2307.

[17] Wang, H.; Yang, Y.; Liang, Y.; Robinson, J.T.; Li, Y.; Jackson, A.; Cui Y.; Dai, H.; Nano Letters, **2011**, 11, 2644.

[18] Wu, S.; Yin, Z.; He, Q.; Huang, X.; Zhou, X.; Zhang, H. The Journal of Physical Chemistry C, **2010**, 114, 11816-11821.

[19] Lin, L. C.; Grossman, J. C. Nature Communications, **2015**, 6, 8335.

[20] Surwade, S. P.; Smirnov, S. N.; Vlassiouk, I. V.; Unocic, R. R.; Veith, G. M.; Dai, S.; Mahurin, S. M. Nature Nanotechnology, **2015**, 10, 459.

[21] Jaafar, H.; Beh, K. S.; Yunus, N. A. M.; Hasan, W. Z. W.; Shafie, S.; Sidek, O. Microsystem Technologies, **2014**, 20, 2109-2121.

[22] Li, P.; You, Z.; Haugstad, G.; Cui, T. (2011). Applied Physics Letters, **2011**, 98, 253105.

[23] Zulkefli, M.; Mohamed, M.; Siow, K.; Yeop Majlis, B.; Kulothungan, J.; Muruganathan, M.; Mizuta, H. Micromachines, **2017**, 8, 236.

[24] Persano, A.; Quaranta, F.; Martucci, M. C.; Siciliano, P.; Cola, A. Sensors and Actuators A: Physical, **2015**, 232, 202-207.

[25] Kalafut, D.; Bajaj, A.; Raman, A. International Journal of Non-Linear Mechanics, **2017**, 95, 209-215.

[26] Shojaei-Asanjan, D.; Bakri-Kassem, M.; Mansour, R. R. Journal of Microelectromechanical Systems, **2019**, 28, 107-113.

[27] Zaghloul, U.; Piazza, G. IEEE Electron Device Letters, **2014**, 35, 669-671.

[28] Chen, Z.; Tian, W.; Zhang, X.; Wang, Y. Journal of Micromechanics and Microengineering, **2017**, 27, 113003.